

Strengthened causal connections between the MJO and the North Atlantic with climate warming

Savini M. Samarasinghe^{3,4}, Elizabeth A. Barnes¹, Charlotte Connolly¹, Imme Ebert-Uphoff^{2,3} and Lantao Sun¹

¹Department of Atmospheric Science, Colorado State University, Fort Collins, CO

²Cooperative Institute for Research in the Atmosphere, Colorado State University, Fort Collins, CO

³Department of Electrical and Computer Engineering, Colorado State University, Fort Collins, CO

⁴Department of Geophysics, Colorado School of Mines, Golden, CO

Corresponding author: Savini M. Samarasinghe (samarasinghe@mines.edu)

Key Points:

- CESM2 captures both the stratospheric and tropospheric pathways connecting the MJO to the North Atlantic
- MJO teleconnections to the North Atlantic strengthen in the future under SSP585 forcing
- The strengthening of the MJO-NAO connection is due to the tropospheric pathway while the stratospheric pathway changes very little

Abstract

While the Madden Julian Oscillation (MJO) is known to influence the midlatitude circulation and its predictability on subseasonal-to-seasonal (S2S) timescales, little is known how this connection may change with anthropogenic warming. This study investigates changes in the causal pathways between the MJO and the North Atlantic Oscillation (NAO) within historical and SSP585 simulations of the CESM2 coupled climate model. Two data-driven approaches are employed, namely, the STRIPES index and graphical causal models. These approaches collectively indicate that the MJO's influence on the North Atlantic strengthens in the future, consistent with an extended jet-stream. In addition, the graphical causal models allow us to distinguish the causal pathways associated with the teleconnections. While both a stratospheric and tropospheric pathway connect the MJO to the North Atlantic in CESM2, the strengthening of the MJO-NAO causal connection over the 21st century is shown to be due exclusively to teleconnections via the tropospheric pathway.

Plain Language Summary

Climate models are useful tools for obtaining better understanding of the complex mechanisms that govern Earth's climate, as well as better understanding of the impacts of climate change. This study focuses on using the newly released Community Earth System Model 2 (CESM2) climate model output along with several data-driven approaches to gain such insights. We focus specifically on the Madden Julian Oscillation (MJO), an atmospheric phenomenon of regions of stormy air and dry air that slowly progresses around the globe in the tropics. The MJO is well known to have an influence on the weather and climate of many parts of the world, including the North Atlantic. Our study finds that the CESM2 climate model correctly simulates connections between the MJO and the North Atlantic and that this influence strengthens over the 21st Century. These insights have important implications for understanding how our ability to forecast weather over Europe and eastern North America may change in the coming decades.

1 Introduction

The Madden-Julian oscillation (MJO) has long been identified as an important source of midlatitude weather predictability on subseasonal-to-seasonal timescales (S2S; approximately 2 weeks to 3 months) via its teleconnections to higher latitudes. Tropical convection associated with the MJO slowly propagates eastward in a quasi-periodic manner, taking approximately 20-90 days to circumnavigate the globe and complete a cycle (Madden & Julian, 1971, 1972; Zhang, 2013). MJO activity can excite Rossby waves which propagate out of the tropics and into the midlatitudes, modifying the large-scale circulation and weather patterns. Because it can take 10-15 days for the teleconnection to reach the midlatitudes, knowing the state of the MJO today can provide information about the evolution of the midlatitude flow in the coming weeks. In fact, multiple studies have demonstrated that the MJO can be used to make skillful forecasts of weather up to 5 weeks in advance across the Northern Hemisphere (Baggett et al., 2017; Cassou, 2008; Mundhenk et al., 2018; Nardi et al., 2020).

While much is known about the MJO and its role in S2S weather prediction, there is substantial uncertainty about how MJO teleconnections may be responding, and will continue to respond, to anthropogenic climate change. Changes can manifest through a combination of changes to the MJO itself and changes to the source and propagation of the Rossby waves into midlatitudes. Focusing first on changes to the MJO itself, Bui and Maloney (2019) show that ratio of MJO-induced circulation to precipitation in CMIP5 climate models decreases as the climate warms, and Hsiao et al. (2020) provide evidence that these changes may already be detectable in the observations. These results are important as they suggest that MJO teleconnections, which are directly excited by the MJO divergent circulation, may weaken as the climate warms (Maloney et al., 2019; Wolding et al., 2017). Thus, the response of the MJO alone to climate warming suggests that skill provided by the MJO could disappear in the coming decades.

Changes in Rossby wave propagation with climate warming are also expected to impact MJO teleconnections. Zhou et al (2020) investigated changes in MJO teleconnections within CMIP5/CMIP6 climate models and demonstrated a robust increase in teleconnections to the west coast of the United States. Their reasoning was that the robust extension of the North Pacific jet-stream changes the Rossby wave propagation paths, acting to shift the teleconnection centers eastward to more directly impact the U.S. west coast. How Rossby wave propagation to the North Atlantic and Europe may change is perhaps more complicated. MJO teleconnections to these regions are known to be dynamically driven by two different pathways, a direct tropospheric pathway and an indirect stratospheric pathway (Barnes et al., 2019). The tropospheric pathway is communicated via tropospheric propagation of Rossby waves from the MJO region to the midlatitudes, which takes approximately 10-15 days (Cassou, 2008; L'Heureux & Higgins, 2008; Lin et al., 2009). The stratospheric pathway instead involves MJO-excited Rossby waves propagating up into the stratosphere and disturbing the stratospheric

polar vortex (a time lag of approximately 15-30 days) (Barnes et al., 2019; Garfinkel et al., 2012, 2014; Kang & Tziperman, 2018; Weare, 2010). It is the signal from the disrupted polar vortex which then propagates downward into the troposphere, impacting the North Atlantic circulation (e.g. M. Baldwin & Dunkerton, 2001; Charlton-Perez et al., 2018; Garfinkel et al., 2014; Kidston et al., 2015). These multiple pathways connecting the MJO to the North Atlantic suggest that changes in teleconnection strength could come about due to changes in Rossby wave propagation through the troposphere, through the stratosphere, stratosphere-troposphere coupling, or changes to the MJO itself.

Here, we investigate how MJO teleconnections to the North Atlantic may change under anthropogenic climate change using 9 historical and 3 SSP585 simulations of the Community Earth System Model, version 2 (CESM2). We invoke two data-driven approaches, namely, the STRIPES index and graphical causal models to quantify MJO teleconnection pathways within CESM2 and how they may evolve with climate warming. These approaches collectively indicate that the MJO's influence on the North Atlantic strengthens in the future and that this change is due exclusively to the tropospheric pathway.

2 Data

2.1 CESM2 simulations

We analyze simulations from the latest generation of the Community Earth System Model (CESM2; Danabasoglu et al., 2020). This coupled climate model is composed of the Community Atmosphere Model version 6 (CAM6), Parallel Ocean Program Version 2 (POP2), CICE version 5.1.2, Community Land Model Version 5 as well as the components of land ice and coupling. CAM6 uses a nominal 1° (1.25° longitude and 0.95° latitude) horizontal resolution configuration with 32 vertical levels with the model top of 2.26 hPa. Changes in CESM2 compared to CESM1 (Hurrell et al., 2013) have resulted in improved historical simulations including major reduction in low-latitude precipitation, and better representation of the MJO and extratropical atmospheric circulation, making it an ideal model for our study (Ahn et al., 2020; Danabasoglu et al., 2020; Simpson et al., 2020).

We analyze data from ensemble members 1, 2, 3, 5, 6, 7, 8, 9, 11 with historical (1850-2014) forcing and ensemble members 4, 10, 11 with SSP585 (2015-2099) forcing. SSP585 represents the high range of possible futures and exhibits an end of century radiative forcing of 8.5 W/m^2 (O'Neill et al., 2016). We focus on daily sea-level pressure, zonal wind at 850 hPa, 250 hPa, and 50 hPa, and precipitation. All fields are re-gridded to a 2° by 2° grid prior to analysis to speed-up computation and reduce data storage. While we center our focus on winter subseasonal variability in December, January and February (DJF), the causal inference approach uses time-shifted/lagged variables that are allowed to extend to November and March as appropriate.

2.2 Climate indices

When computing each of the three climate indices below (i.e. MJO, VORTEX and NAO) every ensemble member and 40-year period are treated completely separately to ensure that the analysis is agnostic to the number of ensemble members available. Prior to any analysis, we remove the 3rd order polynomial trend from each calendar day for each grid point for each field, which removes both the trend over the period and the seasonal cycle. This is done to ensure that all climate indices reflect subseasonal variability, rather than a long-term trend in the mean fields. Ensemble-averages are only performed as a final step prior to plotting the results.

The North Atlantic Oscillation (NAO) is defined as the leading empirical orthogonal function (EOF) of area-weighted monthly-mean SLP anomalies over the region 25N-90N, 90W-30E. The principal components are defined such that a positive value refers to a positive NAO state (low pressure over the poles and high pressure over the mid-North Atlantic) and have been standardized to have a mean of zero and standard deviation of one in Dec.-Feb. NAO sea-level pressure composites from CESM2 are provided in Supp. Figure 1.

The state of the stratospheric polar vortex (VORTEX) is defined as the area-weighted average of anomalous daily 50 hPa zonal wind north of 65N (e.g. Baldwin et al., 1994; Barnes et al., 2019; Charlton-Perez et al., 2018). The index is standardized by subtracting the mean value over DJF and dividing by the standard deviation over DJF for each 40-year period.

The MJO is quantified by the real-time multivariate MJO index (RMM index; Wheeler & Hendon, 2004) defined as the two leading EOFs of meridionally-averaged tropical (15S-15N) anomalous fields of 250 hPa and 850 hPa zonal wind and precipitation. We use model precipitation rather than outgoing longwave radiation (OLR) as is convention since precipitation is more directly simulated by the model. Numerous climate model diagnostics studies use precipitation anomalies to assess MJO simulation skill, and model MJO skill metrics are higher when evaluated with precipitation compared to OLR (Ahn et al., 2017, 2020). In addition to removing the seasonal cycle, we subtract the previous 120-day running mean from each field for each gridpoint to remove any low-frequency modes of variability prior to EOF analysis. Each of the three fields are also standardized by removing the mean and dividing by the standard deviation over all seasons. Supp. Figure 1 shows the structure of the two leading EOFs in the historical and future periods and the historical EOFs compare well with those from observations (Wheeler & Hendon, 2004). The two leading principal components (denoted as RMM1 and RMM2) are standardized to have mean of zero and standard deviation of one. The different phases of the MJO are then defined by the phase space of RMM1 and RMM2 in the conventional way (Wheeler & Hendon, 2004). We define an MJO event as any day where the MJO amplitude ($\sqrt{RMM1^2 + RMM2^2}$) exceeds 0.5.

As has been documented previously, under a warming climate the MJO EOFs shift eastward compared to the historical period in CESM2 due to the eastward extension of tropical Pacific warm sea-surface temperatures (Maloney et al., 2019; Subramanian et al., 2014; Zhou et al., 2020). Due to the shift in the EOFs with warming, we are careful when determining the sign and convention of RMM1 and RMM2 by maximizing the spatial correlation of EOF1 and EOF2 with their historical counterparts.

3 Data-driven approaches

3.1 STRIPES Index

The STRIPES (Sensitivity to the Remote Influence of Periodic EventS) index is designed to capture regional sensitivities to the remote influence of periodic events in a single number (Jenney et al., 2019). Here, we use the STRIPES index to quantify the impacts of the MJO (i.e. magnitude and consistency) on the midlatitude circulation at each midlatitude gridpoint. Specifically, we compute the SLP anomalies 0-35 days following every MJO event of a particular phase. If there is a strong influence of the MJO on that grid point, a tilted stripe will be present in a plot of SLP anomalies as a function of lag (0-35 days) and MJO phase (1-8). A variance calculation of these tilted anomalies produces the STRIPES value, where we focus on tilts that correspond to MJO propagation speeds of 5-9 days per phase. A detailed explanation and visualization of the STRIPES index calculation can be found in Jenney et al. (2019). A higher STRIPES value indicates a larger variance in SLP anomalies, and thus, larger remote influence of the propagating MJO. The ensemble-mean STRIPES index is computed as the average STRIPES value across ensemble members.

3.2 Graphical causal models

Graphical causal models based on Bayesian networks have been successfully used in climate science to gain insights into atmospheric teleconnections (Ebert-Uphoff & Deng, 2012; Kretschmer et al., 2016; Runge et al., 2019) and cross-scale interactions (Samarasinghe et al., 2020), as well as for climate model evaluation (Nowack et al., 2020; Vázquez-Patiño et al., 2020). These approaches provide a compact visual representation of the salient interactions between a set of random variables by representing the variables as nodes of a Directed Acyclic Graph (DAG) and the direct causal relationships between them as arrows/directed edges. In this study we use a temporal extension (Chu et al., 2005; Ebert-Uphoff & Deng, 2012) of the “PC-stable” algorithm (Colombo & Maathuis, 2014; Spirtes et al., 2000) to efficiently derive a DAG from our model data. However, the interactions identified from this data-driven approach (as opposed to targeted simulations) are only *potential* interactions and are *not guaranteed* to be true causal interactions due to reasons such as hidden common causes. Nevertheless, this method provides several advantages over traditional techniques such as correlation analysis and lagged regression by allowing one to easily distinguish direct interactions from indirect ones in a

multivariate setting while still accounting for the memory and feedbacks. See Ebert-Uphoff and Deng (2012) and Samarasinghe (2020), for explanations. Barnes et al. (2019) demonstrated that this causal model approach is capable of distinguishing between the tropospheric and stratospheric pathway of MJO teleconnections to the North Atlantic within observations.

In this study, we derive a temporal DAG by representing the MJO, NAO, and the polar vortex and lagged copies of these variables as separate nodes in a graph. The PC-stable algorithm starts with a fully connected undirected graph initially assuming interactions between every pair of variables, however, instantaneous connections are not allowed. Next, a conditional independence test is used to iteratively disprove the assumed interactions. A pair of variables X and Y cannot have a direct causal connection if they are conditionally independent given any subset of nodes S (excluding X and Y) in the graph. If there is such a subset S , the edge between X and Y is eliminated. We statistically test for zero partial correlation using Fisher's Z -test as the conditional independence test at the 90% confidence level, thus focusing on the average linear dependencies between variables. Finally, we orient the edges such that the interactions are from the past to the future. Our temporal model uses 12 lags each for the MJO, NAO and VORTEX variables with each lag being 5 days apart. We discard one time slice to deal with initialization issues following Ebert-Uphoff and Deng (2012).

To understand how the MJO-NAO teleconnection changes over time, we investigate the interactions identified by PC-stable for each 40-year long window in the historical and future periods, with a 10-year shift between adjacent windows. Prior to the causal analysis, we detrend each 40-year-long NAO and VORTEX time series by removing a first-order polynomial fit of each calendar day and then smooth the data with a 5-day, backward-looking average. We define binary indicator variables for each MJO phase. These variables indicate an MJO event happening in the phase of interest with '1', and '0' otherwise. Unless otherwise noted, we conduct the causal analysis for pairs of phases to increase sample sizes for each group (i.e. phases 2/3, 4/5, 6/7, 8/1).

For each ensemble member, we derive a separate DAG for each 40-year window. We quantify the robustness of each potential causal connection via the "temporal consistency fraction" (tcf) defined below.

$$tcf_{\text{member } i, X \rightarrow Y \text{ at lag } D} = \frac{\# \text{ of times the interaction } X \xrightarrow{D} Y \text{ is in DAG}_i}{\max \# \text{ of times the interaction } X \xrightarrow{D} Y \text{ can occur in DAG}_i}$$

A fraction closer to 1.0 indicates that the interaction is consistently repeating in the temporal model, and thus, robust within that time frame. Figure 3a shows a summary of the potential causal interactions learned by PC-stable that have a tcf of 0.5 or greater for a sample 40-year window of an ensemble member. We average this fraction over the ensemble members as a

metric to distinguish robust causal signals in the CESM2 model while accounting for internal variability. See Supp. Figure 4 for details.

4 Results

Figure 1 compares composites of anomalous sea-level pressure 15 days following MJO phase 7 events between the historical (1850-1889) and future (2055-2094) period for all ensemble members. The SLP teleconnection pattern over the North Atlantic compares well with that observed following MJO phase 7, and represents the negative phase of the NAO (e.g. J. Hurrell, 1995). SLP anomalies increase substantially between the historical and future period, suggesting either stronger or more consistent teleconnections between the MJO and North Atlantic under future climate warming. This strengthening is also present when the two periods are more evenly compared using three ensemble members each (Supp. Fig. 3).

Figure 1 displays results for MJO phase 7 only, however, since the MJO EOFs shift with warming (and thus the phase definitions may too), one would like to know whether the teleconnections are indeed strengthening, or just shifting to a different MJO phase. To quantify the extent to which MJO teleconnections to the NAO *over all MJO phases* strengthen under SSP585, we plot the ensemble-mean STRIPES index for the two periods, and their difference, in Figure 2. Larger STRIPES values imply a larger influence of the MJO on the SLP anomalies there, taking into consideration all phases. The well-known MJO-teleconnection hotspots over the Gulf of Alaska and the North Atlantic are identifiable in both periods (Figure 2a,b) (e.g. Cassou, 2008; Lin et al., 2009; Mori, 2008). While the location of the teleconnection hotspots appear similar between the two periods, the magnitude of the STRIPES index over these hotspots increases substantially by the end of the 21st Century under SSP585 compared to the early historical period (Figure 2c,d). That is, consistent with Figure 1, the STRIPES analysis quantifies a strengthening of the MJO teleconnections with warming, with the largest changes occurring over the Gulf of Alaska and the North Atlantic. While the focus of this study is on the North Atlantic, we return to the North Pacific response in Section 5.

The STRIPES index shows a period of increased values over the North Atlantic in the middle of the 20th century (Figure 2d, pink line), and this mid-century peak is likely related to the strong impact of aerosols on the North Atlantic during this period (Booth et al., 2012). Since the SLP anomalies are detrended by day of year to remove both the seasonal cycle and the long-term trend for each 40-year period, this suggests that the increase in STRIPES is not due to mean change in SLP, but rather, is due to changes in its variability. We will revisit this in the following discussion.

Our results support a strengthening of the teleconnection between the MJO and NAO under SSP585, however, the methodology thus far does not allow us to distinguish between the

tropospheric and stratospheric pathways. To do this, we compute graphical causal models of the MJO, stratospheric polar vortex, and the NAO (see Section 3 for methodology). An example result is shown in Figure 3a for MJO phases 6/7 within a single ensemble member for the 1970-2009 period. Arrows denote potential causal connections between climate phenomena, pointing in the direction of cause to effect, and numbers denote the time lag of the connection in days. Arrows that loop back on themselves signify temporal autocorrelation. The graphical model in Figure 3a demonstrates that CESM2 simulates a direct tropospheric pathway from the MJO to the NAO with a time lag of approximately 15 days following phases 6/7. Furthermore, CESM2 also simulates a stratospheric pathway, evidenced by a connection between the MJO and the VORTEX (time lag of 10-15 days) and then VORTEX to the NAO (time lag of 5 days), resulting in a total time lag of 20 days or so. These connections and time lags are consistent with what is observed over 1979-2016 in reanalyses (Barnes et al., 2019).

Graphs such as that shown in Figure 3a are computed for each 40-year period for each ensemble member for each pair of MJO phases. We summarize the results by computing the temporal consistency fraction (see Section 3) of each connection for each time lag, period and ensemble member, and then average across members. In doing so, we obtain an estimate of the consistency of the causal connection for lags of 5-15 days as a function of time, as shown in Figure 3b. Colored lines denote different causal connections (i.e. arrows in Figure 3a) and it is clear that the direct, tropospheric MJO→NAO connection (pink) substantially strengthens over the 20th and 21st Centuries. The stratospheric pathway, however, shows no evidence of strengthening, with the MJO→VORTEX connection (brown) weakening and then returning to 1800 values, while the VORTEX→NAO connection (green) remains constant over the entire 250 years. That is, the causal models suggest that the changes in MJO teleconnection strength under historical and SSP585 forcings can be attributed exclusively to the tropospheric pathway, with the stratospheric pathway remaining largely unchanged.

Like the STRIPES analysis in Figure 2d, the causal model analysis also shows an increase in teleconnection consistency from the MJO to the North Atlantic in the mid-20th century, but this change is small compared to the changes over the 21st century. This implies that while the magnitude of the North Atlantic SLP anomalies driven by the MJO may have increased over the 1950's (as quantified via STRIPES), the consistency (or robustness) of this direct connection shows the largest increases over the 21st century.

The STRIPES and graphical causal model analyses provide strong evidence of a strengthening of the tropospheric MJO to NAO teleconnection under climate warming within CESM2. At a fundamental level, this could be brought about by (1) a strengthening of the Rossby wave source in the tropics, (2) a strengthening of the wave propagation within the midlatitudes, or both. While a systematic study of the relative importance of each of these mechanisms is outside the

scope of this study, Zhou et al. (2020) suggest that the extension of the North Pacific jet with warming can explain shifts in MJO teleconnections over the western United States in CMIP5 and CMIP6 simulations. We also find a robust extension of the North Pacific and North Atlantic jet-streams within CESM2 (contours in Figure 2c). This extension of the jet-stream from the North Pacific, across North America, and into Europe may enhance the waveguide, supporting Rossby wave propagation from the tropics to the North Atlantic (mechanism #2 above). In fact, changes in the STRIPES index align well with the extensions to the jet, especially over the North Atlantic basin (Figure 2c).

On the other hand, enhancement and shift of the Rossby wave source, for example, through changes in the magnitude and location of MJO heating, could also be at play. While Zhou et al. (2020) focused predominantly on the shift of the MJO teleconnection pattern, their linear baroclinic model experiments suggest that changes in MJO heating alone (a component of mechanism #1) may lead to stronger MJO teleconnections to the North Pacific (their Figure 2d). They did not show results for the North Atlantic. We do find that precipitation anomalies associated with the MJO increase under SSP585 in CESM2 (not shown), so further study is required to truly separate these two mechanisms within the simulations.

5 Discussion and Conclusions

This study is one of the first to provide evidence of strengthened MJO teleconnections to the North Atlantic under SSP585. This result is perhaps surprising, as recent studies have argued that robust increases in tropical static stability may lead to a weakening of MJO teleconnections as the climate system warms (Maloney et al., 2019; Wolding et al., 2017). MJO-to-North Atlantic teleconnections are known to occur via both a stratospheric and tropospheric pathway, and our graphical causal model approach allows us to clearly distinguish between the two. Thus, our results documenting a strengthening of the tropospheric pathway, and theoretical arguments suggesting weakening teleconnections via increased tropical static stability, may be reconciled if the strengthening of the tropospheric pathway is driven predominantly by changes to the waveguide outside of the tropics. To truly disentangle between these competing mechanisms, however, additional model experiments are likely necessary.

The focus of this study was MJO impacts on the North Atlantic, however, our hemispheric STRIPES analysis leaves open questions regarding a strengthening of the MJO-Gulf of Alaska teleconnection in CESM2 (Figure 2). A widening of the North Pacific jet-stream on its polar flank (Figure 2c) may reduce the Rossby wave reflection there and instead be more conducive to wave propagation and breaking (e.g. Ambrizzi et al., 1995). The mechanism behind this change is still not clear to the authors, given that one might expect the extended North Pacific jet to also shift the SLP anomaly eastward, something we do not see in Figure 2. Zhou et al. (2020) find a strengthening of the MJO-induced anomalies in the Gulf of Alaska region when only the MJO

heating is modified to its future state in a linear baroclinic model, yet another possible reason for this response. Thus, further work is needed to understand this Gulf of Alaska response.

Our study employs two data-driven approaches for summarizing and quantifying MJO teleconnections to midlatitudes, and perhaps the methods used in this study are of as much interest as the results themselves. The STRIPES analysis allowed us to summarize many lag and phase diagrams typically used to study MJO teleconnections, while the causal model approach helped disentangle the stratospheric and tropospheric pathways. Both methods provide a straightforward way to compare various teleconnection pathways and strengths within observations and climate models, as well as how the teleconnections may change with time.

Acknowledgements

Work was supported by NSF CAREER AGS-1749261 under the Climate and Large-scale Dynamics program (SS, EB, CC, IE), NSF Award #1934668 of the Harnessing the Data Revolution (HDR) program (IE) and Jim Hurrell's presidential chair startup funding at CSU (LS). The CESM2 CMIP6 datasets are accessible on the Earth System Grid Federation website (historical: doi:10.22033/ESGF/CMIP6.7627; SSP585: doi:10.22033/ESGF/CMIP6.7768).

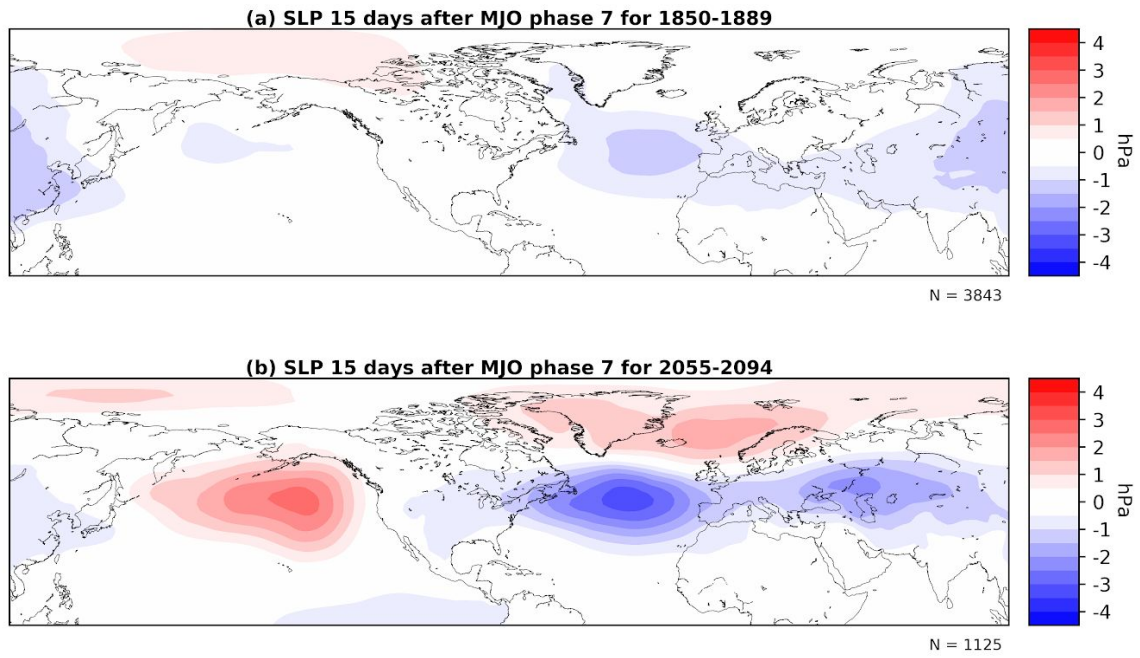


Figure 1: Composite sea-level pressure anomalies 15 days following MJO phase 7 events averaged over ensemble members for the (a) historical (1850-1889; 9 simulations) and (b) future (2055-2094; 3 simulations) periods.

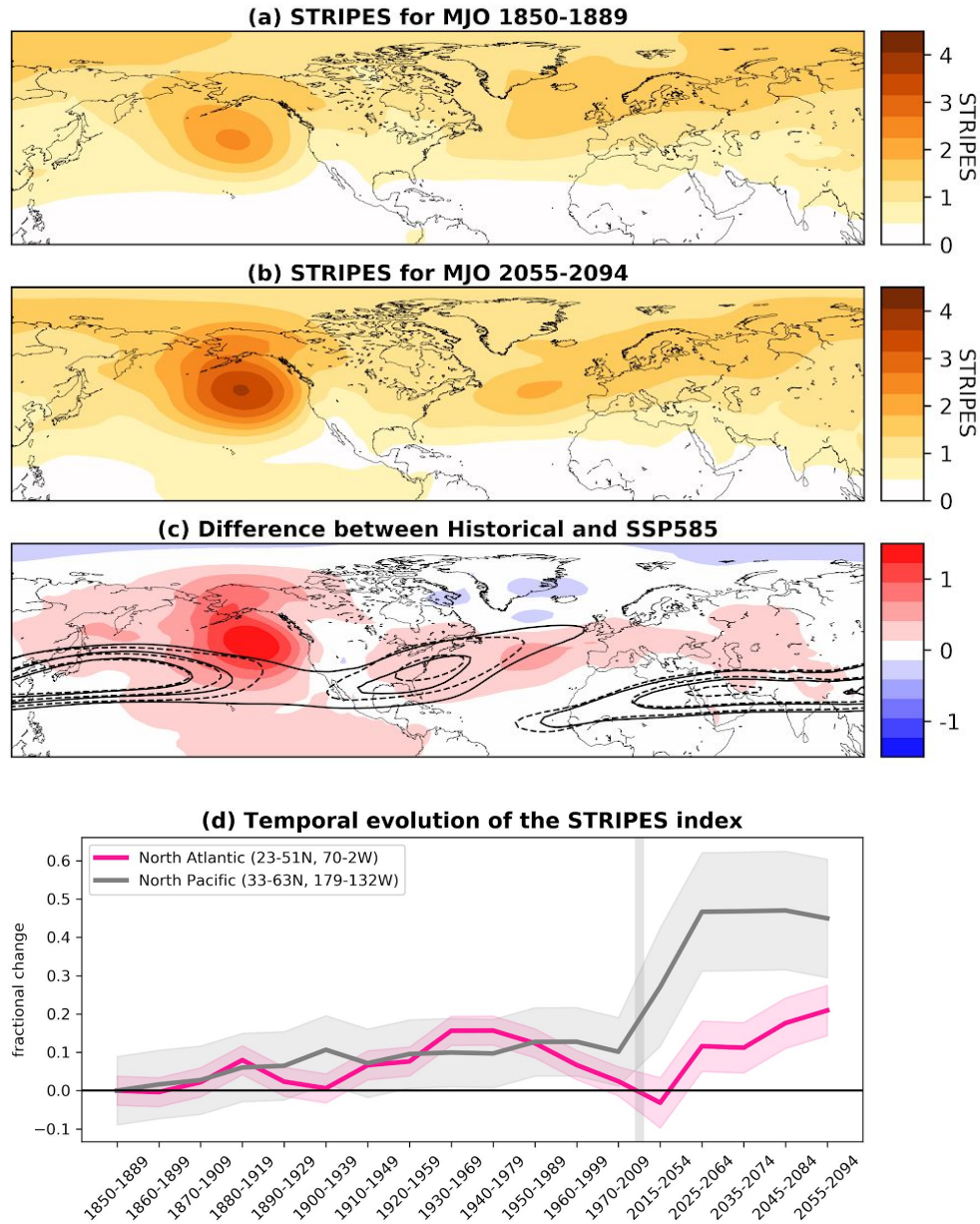


Figure 2: STRIPES values averaged over ensemble members for the (a) historical (1850-1889; 9 simulations) and (b) future (2055-2094; 3 simulations) periods, as well as their (c) difference. Panel (d) displays time series of the regionally-averaged STRIPES, plotted in units of fractional change from 1850-1889. Contours in (c) denote the ensemble-mean 250 hPa zonal winds contoured at 30, 45 and 60 m/s, where dashed and solid lines denote the historical and future periods respectively. Shading in (d) denotes the 90% confidence bounds on the sample mean computed using the 20th century standard deviation across ensemble members. The gray vertical bar denotes a break in the x-axis due to the transition from historical to SSP585 simulations.

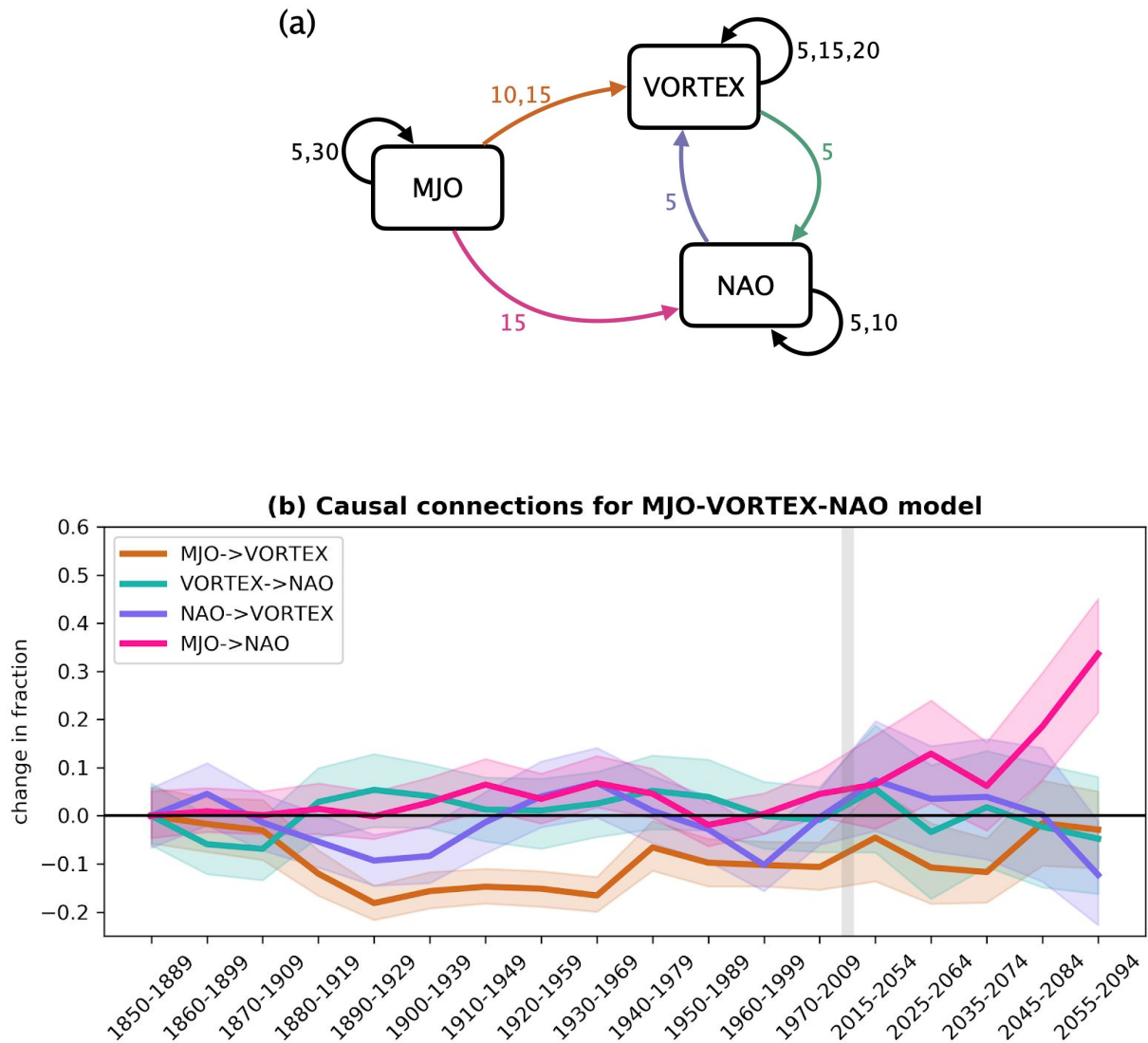


Figure 3: (a) Example graphical causal model for MJO phases 6/7, the VORTEX, and the NAO based on results from historical ensemble member 9 over 1970-2009. (b) Fraction of causal connections relative to the ensemble-mean value in 1850-1889 for causal models of the MJO-VORTEX-NAO. Results are averaged over delays of 5, 10 and 15 days and averaged over all MJO phases and ensemble members. Shading denotes 90% confidence bounds based on Monte Carlo resampling. The gray vertical bar denotes a break in the x-axis due to the transition from historical to SSP585 simulations.

References

- Ahn, M., Kim, D., Sperber, K. R., Kang, I.-S., Maloney, E., Waliser, D., et al. (2017). MJO simulation in CMIP5 climate models: MJO skill metrics and process-oriented diagnosis. *Climate Dynamics*, *49*(11), 4023–4045.
- Ahn, M., Kim, D., Kang, D., Lee, J., Sperber, K. R., Gleckler, P. J., et al. (2020). MJO Propagation Across the Maritime Continent: Are CMIP6 Models Better Than CMIP5 Models? *Geophysical Research Letters*, *47*(11), 741.
- Ambrizzi, T., Hoskins, B. J., & Hsu, H.-H. (1995). Rossby Wave Propagation and Teleconnection Patterns in the Austral Winter. *Journal of the Atmospheric Sciences*, *52*(21), 3661–3672.
- Baggett, C. F., Barnes, E. A., Maloney, E. D., & Mundhenk, B. D. (2017). Advancing atmospheric river forecasts into subseasonal-to-seasonal time scales. *Geophysical Research Letters*, *44*(14), 2017GL074434.
- Baldwin, M., & Dunkerton, T. (2001). Stratospheric harbingers of anomalous weather regimes. *Science*, *294*(5542), 581–584.
- Baldwin, M. P., Cheng, X., & Dunkerton, T. J. (1994). Observed correlations between winter-mean tropospheric and stratospheric circulation anomalies. *Geophysical Research Letters*, *21*(12), 1141–1144.
- Barnes, E. A., Samarasinghe, S. M., Ebert-Uphoff, I., & Furtado, J. C. (2019). Tropospheric and Stratospheric Causal Pathways Between the MJO and NAO. *Journal of Geophysical Research, D: Atmospheres*, *124*(16), 9356–9371.
- Booth, B. B. B., Dunstone, N. J., Halloran, P. R., Andrews, T., & Bellouin, N. (2012). Aerosols

- implicated as a prime driver of twentieth-century North Atlantic climate variability. *Nature*, 484(7393), 228–232.
- Bui, H. X., & Maloney, E. D. (2019). Transient Response of MJO Precipitation and Circulation to Greenhouse Gas Forcing. *Geophysical Research Letters*, 46(22), 13546–13555.
- Cassou, C. (2008). Intraseasonal interaction between the Madden-Julian Oscillation and the North Atlantic Oscillation. *Nature*, 455(7212), 523–527.
- Charlton-Perez, A. J., Ferranti, L., & Lee, R. W. (2018). The influence of the stratospheric state on North Atlantic weather regimes: CHARLTON-PEREZ et al. *Quarterly Journal of the Royal Meteorological Society*, 104, 30937.
- Chu, T., Danks, D., & Glymour, C. (2005). *Data Driven Methods for Nonlinear Granger Causality: Climate Teleconnection Mechanisms*. Carnegie Mellon University.
<https://doi.org/10.1184/R1/6491327.V1>
- Colombo, D., & Maathuis, M. H. (2014). Order-independent constraint-based causal structure learning. *Journal of Machine Learning Research: JMLR*. Retrieved from <http://www.jmlr.org/papers/volume15/colombo14a/colombo14a.pdf>
- Danabasoglu, G., Lamarque, J. -F, Bacmeister, J., Bailey, D. A., DuVivier, A. K., Edwards, J., et al. (2020). The Community Earth System Model version 2 (CESM2). *Journal of Advances in Modeling Earth Systems*. <https://doi.org/10.1029/2019MS001916>
- Ebert-Uphoff, I., & Deng, Y. (2012). Causal Discovery for Climate Research Using Graphical Models. *Journal of Climate*, 25(17), 5648–5665.
- Garfinkel, C. I., Feldstein, S. B., Waugh, D. W., Yoo, C., & Lee, S. (2012). Observed connection between stratospheric sudden warmings and the Madden-Julian Oscillation. *Geophysical*

Research Letters, 39(18), L18807.

Garfinkel, C. I., Benedict, J. J., & Maloney, E. D. (2014). Impact of the MJO on the boreal winter extratropical circulation. *Geophysical Research Letters*, 41(16), 6055–6062.

Hsiao, W.-T., Maloney, E. D., & Barnes, E. A. (2020). Investigating Recent Changes in MJO Precipitation and Circulation in Two Reanalyses. *Earth and Space Science Open Archive*. Retrieved from <https://www.essoar.org/doi/abs/10.1002/essoar.10503998.1>

Hurrell, J. (1995). Decadal trends in the north atlantic oscillation: regional temperatures and precipitation. *Science*, 269(5224), 676–679.

Hurrell, J. W., Holland, M. M., Gent, P. R., Ghan, S., Kay, J. E., Kushner, P. J., et al. (2013).

The Community Earth System Model: A Framework for Collaborative Research. *Bulletin of the American Meteorological Society*, 94(9), 1339–1360.

Jenney, A. M., Randall, D. A., & Barnes, E. A. (2019). Quantifying Regional Sensitivities to Periodic Events: Application to the MJO. *Journal of Geophysical Research, D: Atmospheres*, 124(7), 3671–3683.

Kang, W., & Tziperman, E. (2018). The MJO-SSW Teleconnection: Interaction Between MJO-Forced Waves and the Midlatitude Jet. *Geophysical Research Letters*, 45(9), 4400–4409.

Kidston, J., Scaife, A. A., Hardiman, S. C., Mitchell, D. M., Butchart, N., Baldwin, M. P., & Gray, L. J. (2015). Stratospheric influence on tropospheric jet streams, storm tracks and surface weather. *Nature Geoscience*, 8, 433.

Kretschmer, M., Coumou, D., Donges, J. F., & Runge, J. (2016). Using Causal Effect Networks to Analyze Different Arctic Drivers of Midlatitude Winter Circulation. *Journal of Climate*,

29(11), 4069–4081.

- L’Heureux, M. L., & Higgins, R. W. (2008). Boreal Winter Links between the Madden–Julian Oscillation and the Arctic Oscillation. *Journal of Climate*, 21(12), 3040–3050.
- Lin, H., Brunet, G., & Derome, J. (2009). An Observed Connection between the North Atlantic Oscillation and the Madden–Julian Oscillation. *Journal of Climate*, 22(2), 364–380.
- Madden, R. A., & Julian, P. R. (1971). Detection of a 40–50 Day Oscillation in the Zonal Wind in the Tropical Pacific. *Journal of the Atmospheric Sciences*, 28(5), 702–708.
- Madden, R. A., & Julian, P. R. (1972). Description of Global-Scale Circulation Cells in the Tropics with a 40–50 Day Period. *Journal of the Atmospheric Sciences*, 29(6), 1109–1123.
- Maloney, E. D., Adames, Á. F., & Bui, H. X. (2019). Madden–Julian oscillation changes under anthropogenic warming. *Nature Climate Change*, 9(1), 26–33.
- Mori, M. (2008). The Growth and Triggering Mechanisms of the PNA: A MJO–PNA Coherence. *Journal of the Meteorological Society of Japan*, 86(1), 213–236.
- Mundhenk, B. D., Barnes, E. A., Maloney, E. D., & Baggett, C. F. (2018). Skillful empirical subseasonal prediction of landfalling atmospheric river activity using the Madden–Julian oscillation and quasi-biennial oscillation. *Npj Climate and Atmospheric Science*, 1(1), 7.
- Nardi, K. M., Baggett, C. F., Barnes, E. A., Maloney, E. D., Harnos, D. S., & Ciasto, L. M. (2020). Skillful all-season S2S prediction of U.S. precipitation using the MJO and QBO. *Weather Forecasting*. <https://doi.org/10.1175/WAF-D-19-0232.1>
- Nowack, P., Runge, J., Eyring, V., & Haigh, J. D. (2020). Causal networks for climate model evaluation and constrained projections. *Nature Communications*, 11(1), 1–11.
- O’Neill, B. C., Tebaldi, C., Vuuren, D. P. van, Eyring, V., Friedlingstein, P., Hurtt, G., et al.

- (2016). The Scenario Model Intercomparison Project (ScenarioMIP) for CMIP6. *Geoscientific Model Development*, 9(9), 3461–3482.
- Runge, J., Bathiany, S., Bollt, E., Camps-Valls, G., Coumou, D., Deyle, E., et al. (2019). Inferring causation from time series in Earth system sciences. *Nature Communications*, 10(1), 2553.
- Samarasinghe, S., Deng, Y., & Ebert-Uphoff, I. (2020). A Causality-Based View of the Interaction between Synoptic- and Planetary-Scale Atmospheric Disturbances. *Journal of the Atmospheric Sciences*, 77(3), 925–941.
- Samarasinghe, S. M. (2020). *Causal Inference Using Observational Data-Case Studies in Climate Science* (Doctor of Philosophy). 2020-CSU Theses and Dissertations, Colorado State University.
- Simpson, I. R., Bacmeister, J., Neale, R. B., Hannay, C., Gettelman, A., Garcia, R. R., et al. (2020). An Evaluation of the Large-Scale Atmospheric Circulation and Its Variability in CESM2 and Other CMIP Models. *Journal of Geophysical Research, D: Atmospheres*, 125(13), e2019MS001916.
- Spirtes, P., Glymour, C., & Scheines, R. (2000). *Causation, Prediction, and Search, Second Edition* (Vol. 2nd edition). MIT Press.
- Subramanian, A., Jochum, M., Miller, A. J., Neale, R., Seo, H., Waliser, D., & Murtugudde, R. (2014). The MJO and global warming: a study in CCSM4. *Climate Dynamics*, 42(7), 2019–2031.
- Vázquez-Patiño, A., Campozano, L., Mendoza, D., & Samaniego, E. (2020). A causal flow approach for the evaluation of global climate models. *International Journal of Climatology*,

40(10), 4497–4517.

- Weare, B. C. (2010). Extended Eliassen-Palm fluxes associated with the Madden-Julian oscillation in the stratosphere. *Journal of Geophysical Research*, 115(D24), D24103.
- Wheeler, M. C., & Hendon, H. H. (2004). An All-Season Real-Time Multivariate MJO Index: Development of an Index for Monitoring and Prediction. *Monthly Weather Review*, 132(8), 1917–1932.
- Wolding, B. O., Maloney, E. D., Henderson, S., & Branson, M. (2017). Climate change and the Madden-Julian Oscillation: A vertically resolved weak temperature gradient analysis. *Journal of Advances in Modeling Earth Systems*, 9(1), 307–331.
- Zhang, C. (2013). Madden–Julian Oscillation: Bridging Weather and Climate. *Bulletin of the American Meteorological Society*, 94(12), 1849–1870.
- Zhou, W., Yang, D., Xie, S.-P., & Ma, J. (2020). Amplified Madden–Julian oscillation impacts in the Pacific–North America region. *Nature Climate Change*.
<https://doi.org/10.1038/s41558-020-0814-0>